Characterizing the Response of Lung Tissue in Shear and Indentation Quasi-Static Loading

Madelyn A. K. Eaton, Matthew B. Panzer, Robert S. Salzar

Abstract Pulmonary contusion and other pulmonary injuries can result from common traumas such as motor vehicle crashes, falls or crush injuries, and in military settings such as behind armor blunt trauma. However, injury mechanisms in blunt pulmonary trauma are not well understood for insight into injury prediction. As a starting point for further study, the quasi-static response of lung parenchyma has been characterized using fresh porcine lung, which is structurally comparable to human lung. Shear quasi-static data were used to achieve two constitutive model fits with a single parameter set using the Fung exponential and the Hill Foam models, while indentation quasi-static data were used in validation. Model fit attained with the experimental shear data resulted in a graphically comparable response between the two constitutive models. However, in the indentation validation set, the Fung model had the better fit with sum squared error (SSE) 143, while the Hill Foam model had SSE=762. Though the Fung model was a better fit for quasi-static data, future addition of viscoelastic data may provide a different result with the focus towards later selection of appropriate material models for finite element modeling.

Keywords Biomechanics, Constitutive Modeling, Lung, Material Properties, Quasi-Static.

I. INTRODUCTION

One of the most problematic injury mechanisms associated with blunt thoracic trauma is pulmonary contusion (PC). Problems with this injury type first arise with difficulty of diagnosis. Pulmonary contusion is defined by hemorrhaging into the lung tissue and may peak or plateau as much as 48 hours after initial injury, with respiratory distress peaking as much as 72 hours after initial injury [1]. Furthermore, methods for diagnosis include chest X-ray and CT within the 24-48 hour window following initial injury, and may be overlooked in patients with multiple injuries, seemingly minor injuries, or more severe injuries in locations such as the head. Patients with PC have a higher risk of developing pneumonia and/or acute respiratory distress syndrome (ARDS), and patients with severe cases have an increased likelihood of being treated in the ICU and placed on a ventilator [2-3]. There is also a higher associated morbidity and mortality risk for those diagnosed with PC [4-5].

Blunt injury to the lungs is estimated to occur in up to 75% of patients with blunt thoracic trauma [4], and can occur in a wide range of injurious scenarios with high-energy impact or deceleration. The most common injurious scenario leading to PC is motor vehicle crashes. Second only to head trauma, thoracic trauma in motor vehicle crashes leads to a PC incidence affecting 10–17% of patients admitted to hospital [6]. It was also correlated that occupants younger than 25 years were 50% more likely to sustain PC than older adult occupants (non-elderly) [7]. In a military or in-theater setting, a great incidence of PC occurs in behind armor blunt trauma (BABT). BABT occurs when body armor stops a projectile without penetration, but the armor deforms into the body of the wearer. BABT-like events can occur in both military and civilian scenarios and are a possible cause of PC. If the body armor is not sufficient protection against higher round caliber, then severe PC leading to death can occur [8]. While motor vehicle crashes and BABT are the most commonly reported incidences of PC, it can develop in any injurious scenario involving high-velocity or high-force impacts to the thoracic region (i.e. crush, sports injuries, etc.).

Mechanical testing of lung tissue in non-shockwave incidents has been conceivably sporadic and varied throughout scientific history. There have been multiple experimental tests on blunt impacts to rat lungs and the subsequent models [9-10]. However, there has not yet been any type of scaling configuration from, specifically,

M. A. K. Eaton (e-mail: mak3wd@virginia.edu; tel: 1-434-297-8066) is a PhD student in the Center for Applied Biomechanics at the University of Virginia, USA. M. Panzer and R. S. Salzar are Professors at the Center for Applied Biomechanics in the Department of Mechanical and Aerospace Engineering at the University of Virginia.

blunt-type lung data in rats to human, or to any other small mammal. Thus, we turn to large mammal animal models and other surrogate human models. There have been multiple studies with high-energy impacts on the lungs of live pigs, yet while injury severity response is helpful to the field, no data were reported that could directly translate into material properties and damage thresholds for modeling purposes [11-13]. The most-used large mammal lung properties dataset has actually come from large breed dogs. Particularly, the experiments conducted by Vawter *et al*. [14] loads dog lung in uniaxial and biaxial tension, resulting in an elastic modulus and stress/strain curves. As far as the literature is concerned, no other studies attempted to replicate this tensile lung testing on any large mammal models, yet [14] has been used as a source of experimental data for use in many constitutive models. The complexity of the models developed directly from the dog lung data varies in complexity and usability, and despite uses by smaller projects and research, none of the most popular whole body finite element human body models have adopted them as their material model for lung [15-17]. One of the most important large mammal model testing with respect to the current work has been a porcine lung isotropy study done with uniaxial compression. Experimental and histological analysis showed no statistical difference between the three testing planes – frontal, sagittal and transverse – concluding that lung is an isotropic material [18].

There have been three forms of postmortem human specimen (PMHS) testing for the material properties of lungs. One of these is a test using a Kolsky bar technique. A Kolsky bar setup is a testing mechanism originally designed for testing metals under high strain rate, and its usage is not entirely proven to be effective for extremely soft materials such as the lung due to the exceptionally low stiffness of the lung material and the high stiffness of the metal pistons. The low stiffness specimen is also usually completely destroyed in the course of the test with high strain rates not realistic of in-vivo loading. Regardless, PMHS lung bulk and shear moduli were reported along with stress/strain curves for varying strain rates [19]. Another study includes uniaxial tensile PMHS experimentation with over half of the PMHS population tested having some sort of chronic lung disease (e.g. cancer, emphysema, tuberculosis). The focus of this study seemed more towards highlighting the difference in tensile properties in diseased lung, although some of the curves reported are non-diseased lung for comparison [20]. Finally, perhaps the most important study in relation to the current work is a thorough biaxial tensile testing of PMHS lung [21]. This study gives useful data in Lagrangian stress and strain as well as creep and relaxation curves for rectangular, previously-frozen lung samples under biaxial tension through silk thread. The study goes on to fit a constitutive model to the data based on a strain energy density function developed by Fung [22]. There is also a comparison between biaxial testing of dog lung [14] and PMHS lung [21]. Zeng *et al*. [21] concludes that: for dog lung to develop the same stress, it needs to stretch more at lower stress levels. At the same stretch ratio, PMHS lung tissue develops more stress than dog. And, in model fitting, the constant, which determines overall stress level, is three times smaller in dogs, showing that PMHS lung is stiffer than dog lung.

No quasi-static lung data were found in the literature for large mammal models nor was there non-Kolsky bar shear data at any type of strain rate. Therefore, for the current experimental work it was decided to create a quasi-static basis in order to fill the partial gap in literature and inform material models. Fresh, never frozen, porcine lung was chosen for this study for its closeness to human lung. Preliminary testing in relation to this study has suggested that the material properties of non-smoker human lung tissue lie within the standard deviation of porcine lung material properties. Size and weight of whole lungs, as well as alveoli size, are comparable in humans and porcine specimens. Furthermore, xenogeneic cross-circulation studies have proven that human lung can remain viable in a porcine specimen, and an expansion on the results of those studies could prove the opposite assumption true [23]. So for the context of this experimental work, it is at this point assumed a 1:1 *structural* correlation between human and pig for mechanical testing purposes only, the former relation being untrue for any type of biochemical relation.

This work will be the first of its kind focusing on quasi-static lung properties of a large animal model. The two proposed modes of testing will be in shear and cylindrical indentation. Two constitutive models will be fitted to the shear experimental data, and the indentation experimental data will be used for model validation. Like [21], this study will use a Fung model as one of the chosen constitutive models, though a more simplified version to better include the addition of viscoelasticity at a future time. The other will be a Hill Foam model, chosen for its representation of very soft materials. The specific constitutive models were also chosen to help pave a clear path for an easy transition to a viscoelastic model fitting, with the addition of viscoelastic data, and ease of input into a material model for finite element analysis.

II. METHODS

This study is comprised of both experimental testing on small-scale samples of porcine lung parenchyma, and constitutive modeling from the resulting output of the experimental testing. This allows for a comprehensive understanding of the material properties associated with lung while giving insight into future computational modeling strategies. There are two separate methodologies to this approach: experimental testing and constitutive modeling, both described below.

Experimental Testing

Fresh porcine lung was acquired ~1 hour after sacrifice from a meat processor (T&E Meats, Harrisonburg, VA), and all testing was completed within 24 hours after sacrifice. In all, ten fresh porcine lung specimens were tested, each with six samples extracted – three samples for shear and three for indentation. This study defines *specimens* as separate animal subjects and *samples* as pieces taken from those animal subjects: i.e. there are multiple samples originating from one specimen. Since lung parenchyma has been determined to be isotropic [18], samples were taken from the mid-lobe region from both the left and right lung's largest lobe. Care was taken to insure no bronchiole were included in the sample. For future modeling purposes, lung is assumed to be homogeneous on the macroscale. Rectangular shear samples were cut from the whole lung so that only lung parenchyma was excised. For this reason, sample thickness had a slight variation. Likewise, cylindrical indentation samples were cut from the lung parenchyma for cylindrical indentation testing. All samples were tested within two hours of being cut from the whole lung specimen, and at intervals a saline solution was atomized into the air above the lung samples to represent an in-vivo level of moisture. In order to achieve an accurate thickness measurement of the cylindrical indentation samples, a thin needle was inserted through the thickness, marked, and then the measurement attained by calipers. The thin needle insertion did not change the material response of the lung samples. The diameter of the indentation samples and the measurements of the shear samples were reached through direct measure with calipers, and the average sample measurements can be seen in Table I.

All sample testing was done using a displacement driven bench-top test machine (ElectroForce® 3100, Bose Corporation – ElectroForce, Eden Prairie, MN) along with a 1000 g load cell. The shear setup consisted of two aluminum shearing plates aligned vertically, one connected to the load cell and the other to the test machine's actuator (Fig. 1a). Shear samples were fixed to the shearing plates using a thin layer of glue (Loctite®, Henkel Corporation, Westlake, OH) so that the thickness was the span between the shearing plates. The glue allowed for rigid fixture of the samples to the plates to avoid friction or slipping. The samples were then sheared in a quasi-static manner at 0.05 mm/s for 220 s. The indentation samples were placed on an aluminum plate connected to the load cell and uniaxially compressed with a cylindrical indenter (Fig. 1b). The indentation samples' radii were determined such that when the 6.36 mm cylindrical indenter was used, the infinite half-plane scenario was maintained. The indentation samples were compressed in a quasi-static manner at 0.05 mm/s for 120 s. Both of these testing mechanisms resulted in force and displacement time histories.

TABLE I
AVERAGE SAMPLE MEASUREMENTS FOR SHEAR (LEFT) AND INDENTATION (RIGHT) SAMPLES.
THICKNESS REFERS TO THE TESTING PLANE (E.G. FOR SHEAR IN BETWEEN THE SHEAR PLATES)

(mm)	**Shear (n=30)**
thickness	7
length	8.5
width	7.3

(mm)	**Indentation (n=30)**
thickness	9.5
diameter	33.8

Shear Test Setup

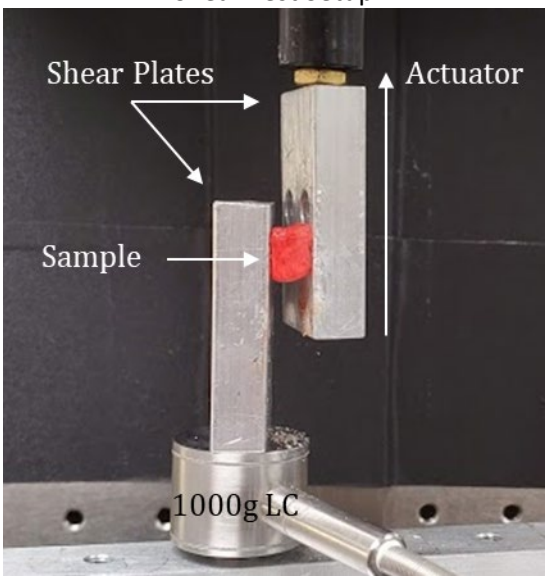

Fig. 1a. – The shear experimental test setup is depicted. A sample is fixed to two shearing plates, the rightmost of which is connected to the actuator. The leftmost shear plate is connected to a 1000 g load cell (LC).

Indentation Test Setup

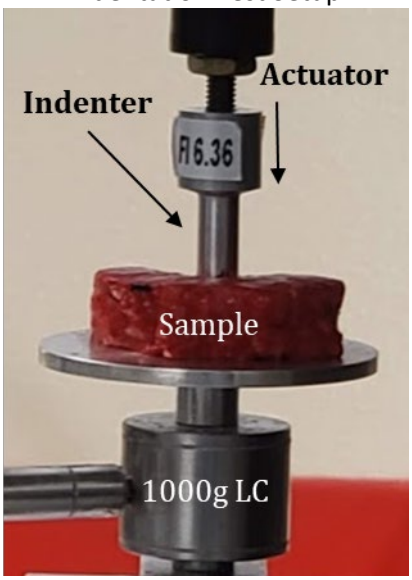

Fig. 1b. – The indentation experimental test setup is depicted. The sample sits on a circular aluminum platen connected to a 1000 g load cell (LC). A cylindrical indenter is connected to the actuator.

Constitutive Modeling

Once the force and displacement time histories from the experimental testing were attained, engineering stress and engineering strain (Lagrangian) were calculated using the initial measurements of individual samples. Data from each sample were averaged with the other samples from a specific specimen, creating an averaged curve per specimen per test type. These specimen curves were then used to achieve single characteristic experimental curves for both sets of test types through methods found in [24]. The characteristic experimental curve for quasi-static shear was used for constitutive modeling, while the characteristic quasi-static indentation curve was used for validation. Two constitutive models were fit for comparison: the Fung exponential model [25] and the Hill Foam model [26-27].

The constitutive model types were picked to fit a form that would later be used with the addition of viscoelastic data. The viscoelastic modeling form, in particular, is quasi-linear viscoelastic (QLV) fitting, and models the stress response to an arbitrary strain input:

$$\sigma(\varepsilon,t) = \int_0^t G(t-t')\frac{\partial \sigma^e(\varepsilon)}{\partial \varepsilon}\frac{\partial \varepsilon}{\partial t'}dt' \quad (1)$$

where σ is stress, ε is strain, t is time, $G(t)$ is the reduced relaxation function, and $\sigma^e(\varepsilon)$ is the instantaneous elastic response (IER). The goal of the current study is to fit the quasi-static data to the IER. For the Fung exponential model that takes the form of:

$$\sigma(\varepsilon) = A[e^{B\varepsilon} - 1] \quad (2)$$

where A and B are parameters to be fitted to the data. The Hill Foam IER was developed with the Hill Foam strain energy density function under the assumption of simple shear (the Jacobian J=1):

$$\sigma(\varepsilon) = C\frac{\partial \lambda}{\partial \varepsilon}\frac{(\lambda^{2b}-1)}{\lambda^{b+1}} \quad (3)$$

where C and b are parameters to be fitted and λ is the stretch defined in this particular case (geometrically) as:

$$\lambda = \sqrt{\varepsilon^2+1} + \varepsilon \quad (4)$$

The fits of the two possible IERs were determined by minimizing the sum squared error (SSE) between the characteristic experimental shear curve and the predicted model fitting (Excel Solver®, Microsoft®, Redmond,

WA). Each of the possible IERs were fit using a single set of parameters. After attaining the model fits for the shear data, the Fung exponential and the Hill Foam model were then compared to the characteristic experimental indentation curve for verification of fit for quasi-static lung data.

III. RESULTS

All ten porcine specimens produced samples that were successfully tested and had no visible inconsistencies, either structurally or in graphical data, that would suggest obvious failure of material. Further, there were no observed differences between samples taken from the right or left lung, and extraction location of samples was consistent throughout the specimens. Figures 2 and 3 depict the engineering stress vs. time curves per specimen for quasi-static shear and indentation, respectively. It should be noted that in the time history curves, the difference in sample thickness is not yet accounted for, which leads to a spread in the observed engineering stress. In order to properly achieve a model fit for the quasi-static shear data, a characteristic experimental curve was found. This characteristic experimental curve was derived using an average of the specimens that accounted for different end-point strains. Strain was first normalized for all specimens by dividing by peak strain, then the data interpolated as to have common normalized strain. This results in all curves having stress values at common strain points. The data can then be averaged point-by-point, then the average multiplied by the specimen averaged peak strain to result in the characteristic experimental curve. This technique was chosen due to its known usefulness in the field when dealing with more complex testing [24]. In Fig. 4 the characteristic experimental shear curve can be seen along with corridors denoting the standard deviation.

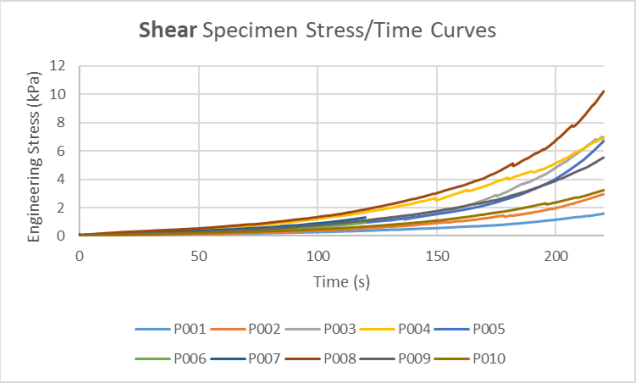

Fig. 2. – The engineering stress (kPa) vs time (s) for the averaged specimen curves for the quasi-static shear testing. It should be noted that differences in sample thickness are unaccounted for, causing a false perspective on the spread of the data.

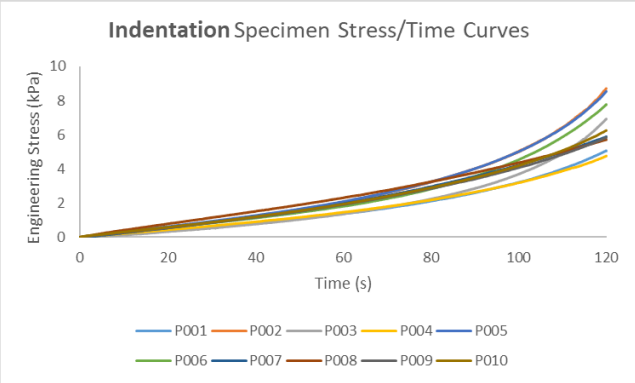

Fig. 3. – The engineering stress (kPa) vs time (s) for the averaged specimen curves for the quasi-static indentation testing. See note on Fig. 2.

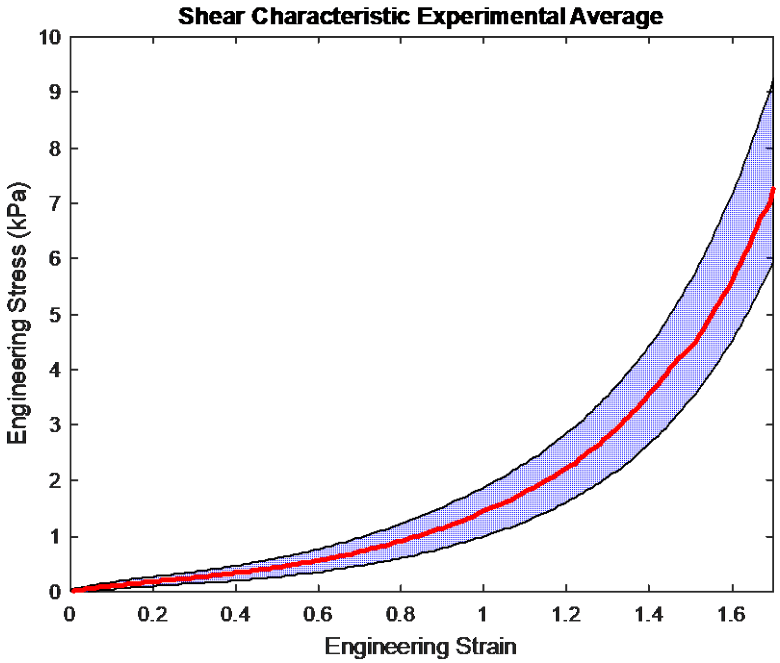

Fig. 4. – The characteristic experimental curve for the averaged quasi-static shear data (bolded red line) and the standard deviation corridor (shaded region) with the x-axis being engineering strain, and the y-axis engineering stress (kPa).

Once the characteristic experimental shear curve was defined, it was used to solve for model fits for both the Fung exponential model and the Hill Foam model as possible IERs for later QLV characterization. The parameters gained from the model fitting can be viewed in Table II. The graphical results for both model fits to the shear quasi-static data can be seen in Fig. 5. As seen in Fig. 5a, both model fits have visual closeness to the experimental curve, yet the Fung model comes slightly closer than the Hill Foam model (Fig. 5b). The difference in closeness of fit between the two possible constitutive models becomes more apparent when the experimental indentation data are taken into account. This can be seen in Fig. 6, where the characteristic experimental indentation curve is fitted to the two models using the parameters from the shear fitting. How the models represent the experimental indentation data is an example of goodness of fit validation, since the model parameters were realized using only the experimental shear data. This is also expressed in Table III, which details the R-squared and SSE values for the fitting seen in Fig. 5 and Fig. 6.

TABLE II

THE VALUES OF THE MODEL PARAMETERS THAT WERE FITTED TO THE EXPERIMENTAL DATA. ON THE LEFT SIDE ARE THE PARAMETERS C (CONSTANT) AND B (EXPONENT) FROM THE POSSIBLE HILL FOAM IER, AND ON THE RIGHT SIDE ARE THE PARAMETERS A (CONSTANT) AND B (EXPONENT) FROM THE POSSIBLE FUNG IER

Hill Foam Parameters		Fung Parameters	
C	0.0391	A	0.180
b	4.42	B	2.14

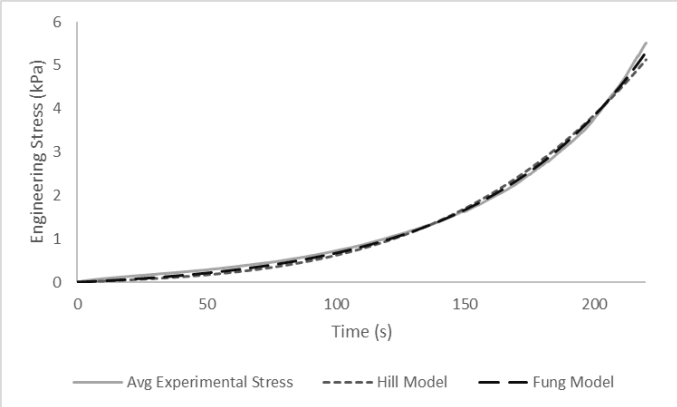

Fig. 5a. – The engineering stress (kPa) vs. time (s) curve for the shear experimental average (solid gray), the Hill Foam model fit (dotted), and the Fung exponential model fit (dashes).

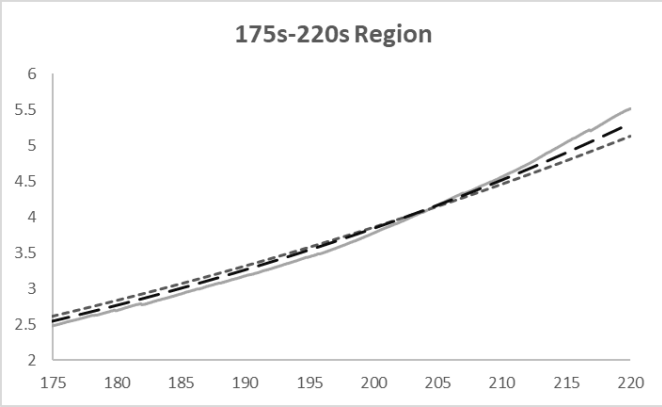

Fig. 5b. – A close-up of Fig. 5a for the 175–220 seconds region. Y-axis is in engineering stress (kPa), x-axis in time (s).

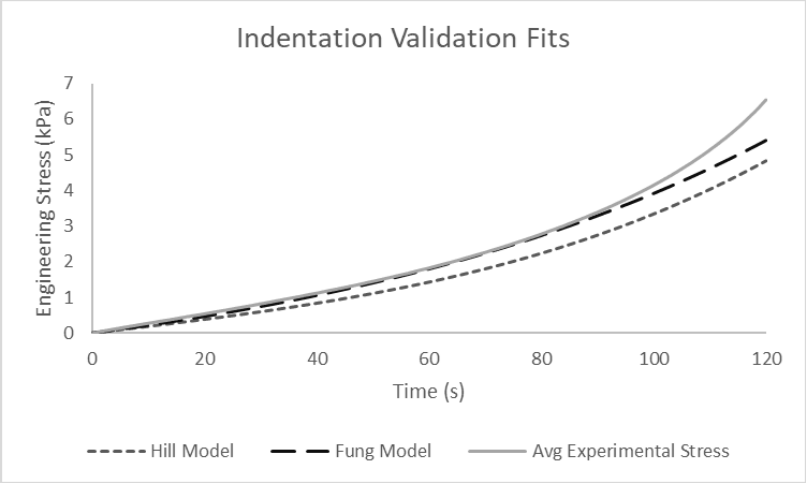

Fig. 6. – The characteristic experimental indentation curve (solid gray), plotted alongside the Hill Foam model (dotted) and the Fung exponential model (dashed) using the parameters from the shear fit.

TABLE III
THE R^2 AND SSE VALUES FOR THE EXPERIMENTAL SHEAR (FIRST ROW) AND EXPERIMENTAL INDENTATION (SECOND ROW) DATA FITTED TO THE HILL FOAM (LEFT) AND FUNG (RIGHT) MODELS

	Hill Foam Model		**Fung Exponential Model**	
	R^2	SSE	R^2	SSE
Shear:	0.9951	71.00	0.9984	24.30
Indentation:	0.9978	761.82	0.9924	143.11

IV. DISCUSSION

The properties of lung tissue have not been widely studied, and there is a distinct lack of mechanical testing data within the literature. This study's purpose was to help fill the gap within literature with a quasi-static baseline for further computational modeling. Experimental engineering stress and strain values were obtained for both testing in shear and cylindrical indentation of fresh porcine lung parenchyma. The standard deviation corridor expressed in Fig. 4 for the experimental shear data indicates that the quasi-static response of lung tissue in shear falls within a narrow margin, suggesting that the full scope of quasi-static material properties can be properly achieved. Two constitutive models were chosen to characterize the material properties of lung, a Fung exponential model and a Hill Foam model, both in a form that could later be used as IERs for QLV fitting. When using the characteristic experimental shear curve to fit the models' parameters, both models achieved a good fit with the experimental data (SSE<100). The fitting of the models' parameters is based upon minimizing the SSE,

and thus are fit to local, not necessarily global, minima. As a result, replicating the model fittings may produce slightly different numbers and SSE values. To make sure the model fits have an appropriate local minima value (i.e. fitting multiple times will result in parameters within a standard deviation), each curve averaged per specimen was also fit. The individual specimen fits resulted in parameters within a standard deviation of the characteristic experimental curve fit, concluding that the model parameters gained for shear were viable. At this stage, neither model was significantly better than the other at representing the experimental data. For model validation, the characteristic experimental indentation curve was fit to each model using the parameters gained through shear. This resulted in a more recognizable difference between the two models: the Fung fit had SSE=143, and the Hill Foam SSE=762. The Fung exponential possible IER seems to be a better fit for this case of a single parameter set. However, the addition of multiple parameter sets (e.g. C_1 and b_1, C_2 and b_2) could sway the results in favor of another model.

As this particular experimental data set is a new addition to the literature, it is difficult to directly compare the results in the context of other studies done on the material properties of lungs. Perhaps the simplest comparison measure would be the elastic modulus that has been reported for various types of testing mechanisms [14][19][28], but due to the quasi-static nature of the current study this comparison cannot be made. With the later accrual of viscoelastic experimental data to complete the QLV characterization, the elastic moduli determined from that testing will be a telling factor in comparability of the older literature data. Even though [21] dealt with biaxial tensile data, in a uniaxial tension test performed with cyclic loading of 0.04 Hz an engineering stress/strain curve of the loading phase was produced. This engineering stress/strain curve of the loading phase had similar curve shape to the quasi-static data of the current study. Furthermore, a stress of 2 kPa was a resultant of a strain of approximately 1.45 in [21] and 1.15 in the current study. A Fung-type constitutive model was discovered through optimization of the SSE as well. The five previously-frozen PMHS specimens were optimized separately, and a good fit was obtained for each with SSE between 3.39 and 1001 [21].

There are certainly limitations in the field of injury biomechanics, and this work is no exception. Perhaps the most obvious limitation is the lack of in-vivo testing. PC is defined as bleeding into lung parenchyma, and sacrificed porcine material has no such ability. For this reason, all testing in this work was kept at reasonably low strain levels well under the theorized failure point of lung tissue. The other large issue with ex-vivo testing is replicating the in-vivo environment while testing the samples. Attempted replication of moisture and salinity levels with repeated misting of a saline solution helped to bridge this gap; however, all testing was done at room temperature. It should also be noted that the exercised state of the lung tissue at times of blunt injury can vary in field (i.e. inhalation or deflation). Paired with difficulties in laboratory experimentation, the decision in regard to this issue was to test lung parenchyma in an 'equilibrium' state: neither deflated nor inflated, but rather solely supported by the relaxed state of the structural material. This state allows for allocation of the characterization of properties in a purely structural sense of the material, without the worry of pre-stressed states due to air volume. Nonetheless, the lungs do have multiple types of pre-stressed states within the activity of breathing which are difficult to replicate in experiment, and are not represented within this test series.

Another limitation to be addressed is the inconsistencies of measurement in engineering stress and strain. Engineering strain measures rely on the consistency of experimental measurement, which may be a source of error especially in very soft materials. Engineering stress measures as a result of the experimental testing may not be representative of all parts of the sample. In shear testing, for example, the stress state in the middle of the sample may not match the stress state at the shearing edge of the sample, and both of these stress states may not match the engineering stress measure gained from the output force. This inconsistency may be seen in later computational modeling of lung material.

V. CONCLUSIONS

Quasi-static lung response data were readily achieved in both shear and indentation loading using fresh porcine lung. Thus, the full scope of lung material properties could be identified with the addition of viscoelastic data. Aiding in this identification is the constitutive modeling through parameter fitting of the experimental results. Of the two constitutive models explored, the Fung exponential model achieved a better fit than the Hill Foam model to the experimental shear data when fitting with a single set of parameters. However, this does not necessarily conclude that the Hill Foam would not be the best choice for finite element analysis, as there are many other factors contributing to computational model success. Nonetheless, the constitutive modeling of this quasi-static

lung data properly prepares the path towards constitutive fitting of viscoelastic properties through the use of QLV and the possible IER functions discussed in this work.

VI. REFERENCES

[1] Cohn, S. M. (1997) Pulmonary contusion: review of the clinical entity. *The Journal of Trauma: Injury, Infection, and Critical Care*, **42**(5): pp.973–979.

[2] Miller, P. R., Croce, M. A., *et al*. (2001) ARDS after pulmonary contusion: accurate measurement of contusion volume identifies high-risk patients. *The Journal of Trauma: Injury, Infection, and Critical Care*, **51**(2): pp.223–230.

[3] Ho, S. W., Teng, Y. H., *et al*. (2016) Risk of pneumonia in patients with isolated minor rib fractures: a nationwide cohort study. *BMJ Open*, **7**(1): pp.1–8.

[4] Miller, C., Stolarski, A., *et al*. (2019) Impact of blunt pulmonary contusion in polytrauma patients with rib fractures. *The American Journal of Surgery*, **218**(1): pp.51–55.

[5] Alisha, C. (2015) Risk factors affecting the prognosis in patients with pulmonary contusion following chest trauma. *Journal of Clinical and Diagnostic Research*, **9**(8): pp.17–19.

[6] Gayzik, S. F., Martin, S. R., *et al*. (2009) Characterization of crash-induced thoracic loading resulting in pulmonary contusion. *The Journal of Trauma: Injury, Infection, and Critical Care*, **66**(3): pp.840–849.

[7] O'Connor, J. V., Kufera, J. A., *et al*. (2009) Crash and occupant predictors of pulmonary contusion. *The Journal of Trauma: Injury, Infection, and Critical Care*, **66**(4): pp.1091–1095.

[8] Gryth, D., Rocksen, D., *et al*. (2007) Severe lung contusion and death after high-velocity behind-armor blunt trauma: relation to protection level. *Military Medicine*, **172**(10): pp.1110–1116.

[9] Raghavendran, K., Davidson, B., *et al*. (2005) A rat model for isolated bilateral lung contusion from blunt chest trauma. *Anesthesia & Analgesia*, **101**(5): pp.1482–1489.

[10] Bel-Brunon, A., Kehl, S., Martin, C., Uhlig, S., Wall, W. A. (2014) Numerical identification method for the non-linear viscoelastic compressible behavior of soft tissue using uniaxial tensile tests and image registration – application to rat lung parenchyma. *Journal of the Mechanical Behavior of Biomedical Materials*, **29**: pp.360–374.

[11] Wang, N., Stevens, M. H., Doty, D. B., Hammond, E. H. (2003) Blunt chest trauma: an experimental model for heart and lung contusion. *The Journal of Trauma: Injury, Infection, and Critical Care*, **54**(4): pp.744–749.

[12] Magnan, P., Sarron, J. C., *et al*. (2004) Physiological results of French BABT experiments – comparison with non lethal kinetic weapons. *Proceedings of Personal Armour Systems Symposium (PASS)*, 2004.

[13] Rater, J. F. (2013) Thorax soft tissue response for validation of human body models and injury prediction. *Chalmers University of Technology*, 2013, Gothenburg, Sweden.

[14] Vawter, D. L., Fung, Y. C., West, J. B. (1978) Elasticity of excised dog lung parenchyma. *The American Physiological Society*, pp.261–269.

[15] Wang, H. K., Yang, K. H. (1995) The development of a finite element human thoracic model. *Proceedings of 5th Injury Prevention Through Biomechanics Symposium*, 1995.

[16] Clayton, J. D., Freed, A. D. (2020) A constitutive model for lung mechanics and injury applicable to static, dynamic, and shock loading. *Mechanics of Soft Materials*, **2**(1): pp.1–35.

[17] Yuen, K., Cronin, D. S., Deng, Y. C. (2008) Lung response and injury in side impact conditions. *Proceedings of International Research Council on Biomechanics of Injury (IRCOBI) Conference*, 2008, Bern, Switzerland.

[18] Weed, B., Patnaik, S., *et al*. (2015) Experimental evidence of mechanical isotropy in porcine lung parenchyma. *Materials*, **8**(5): pp.2454–2466.

[19] Saraf, H., Ramesh, K. T., Lennon, A. M., Merkle, A. C., Roberts, J. C. (2007) Mechanical properties of soft human tissues under dynamic loading. *Journal of Biomechanics*, **40**(9): pp.1960–1967.

[20] Sugihara, T., Martin, C. J., Hildebrandt, J. (1971) Length-tension properties of alveolar wall in man. *Journal of Applied Physiology*, **30**(6): pp.874–878.

[21] Zeng, Y. J., Yager, D., Fung, Y. C. (1987) Measurement of the mechanical properties of the human lung tissue. *Journal of Biomechanical Engineering*, **109**: pp.169–172.

[22] Fung, Y. C., Tong, P., Patitucci, P. (1978) Stress and strain in the lung. *Journal of the Engineering Mechanics Division*, pp.200–223.

[23] Hozain, A. E., O'Neill, J. D., *et al*. (2020) Xenogeneic cross-circulation for extracorporeal recovery of injured human lungs. *Nature Medicine*, **26**(7): pp.1102–1113.

[24] Lessley, D., Crandall, J., Shaw, G., Kent, R., Funk, J. (2004) A normalization technique for developing corridors from individual subject responses. *Proceedings of SAE World Congress & Exhibition*, 2004.

[25] Fung, Y. C. (1993) *Biomechanics: Mechanical Properties of Living Tissues*. Springer: New York, NY, pp.277–280.

[26] Hill, R. (1978) Aspects of invariance in solid mechanics. *Advances in Applied Mechanics*, **18**: pp.1–75.

[27] Storåkers, B. (1986) On material representation and constitutive branching in finite compressible elasticity. *Journal of the Mechanics and Physics of Solids*, **34**(2): pp.125–145.

[28] Sundaram, S. H., Feng, C. C. (1977) Finite element analysis of the human thorax. *Journal of Biomechanics*, 10(8): pp.505–516.